Localized defect modes in a two-dimensional triangular photonic crystal

Vladimir Kuzmiak*
Research Institute for Electronic Science, Hokkaido University, Kita-ku, Sapporo 060, Japan

Alexei A. Maradudin
Department of Physics and Astronomy, University of California, Irvine, California 92697
(Received 20 October 1997; revised manuscript received 2 March 1998)

By using a finite-difference time-domain numerical method based on introducing an oscillating dipole at a proper position in a two-dimensional photonic crystal consisting of an array of dielectric cylinders, we numerically solve the inhomogeneous wave equation discretized in both space and time to calculate the eigenfrequency and the eigenfunction of a localized defect mode. We study the spatial distribution of the electric field and the radiated power associated with the defect modes produced by introducing a defect cylinder into an otherwise periodic two-dimensional triangular photonic crystal. We have obtained excellent agreement for the defect mode of A_1 symmetry created by removing a single cylinder from the center of the region of cylinders arrayed in a triangular lattice with the experimental result of Smith *et al.* [J. Opt. Soc. Am. B **10**, 314 (1993)]. We have also examined systems in which defect states are introduced by varying the radius of a single cylinder and when both the dielectric strength and the radius of the defect cylinder are changed. The calculated values of the donor and acceptor levels associated with the exponentially decaying defect modes of A_1 symmetry induced by changing the radius are in good quantitative agreement with the nondegenerate donor and acceptor levels obtained by the supercell method within the plane-wave approach reported recently by Feng *et al.* [Jpn. J. Appl. Phys. **36**, 120 (1997)].
[S0163-1829(98)05324-7]

I. INTRODUCTION

Since the discovery of a new class of periodic dielectric structures—photonic crystals[1,2]—considerable progress has been achieved in exploring the nature of these artificially created materials[3,4] that possess unique physical properties such as the existence of photonic band gaps[5] and the localization of light in the presence of disorder,[2] which may lead to applications in many scientific and technical areas.[6]

One of the most intriguing properties of photonic band-gap crystals is the emergence of exponentially decaying localized defect modes that may appear within the photonic band gaps when a defect is introduced into an otherwise perfect photonic crystal.[1,7–23] Understanding the nature of the localized modes and determining the conditions under which photon bound states exist within the gaps is of particular importance for various potential applications of doped photonic crystals in semiconductor lasers, resonators, and frequency filters. The calculations of the frequencies and the fields associated with these defect modes were performed by using supercell methods,[10,12–15,18,22,23] which are based on computer simulation methods, and by exact Green's function methods,[16,17,19,20] which yield the solution of the impurity problem in terms of the eigenvalues and eigenfunctions of the photonic band structure of the perfect photonic crystal.

A supercell method in which a single defect is placed in a repeated cell of a sufficiently large size introduces an array of defects into the structure rather than just a single defect. The overlap between the modes localized at the defects in the neighboring cells gives rise to a dispersion of the impurity band, and the frequency of the band is taken to be the band center. As alternative exact methods for studying the localized modes in photonic crystals, schemes based on the application of the Green's-function formalism have been developed.[16,17,19,20] In an approach presented by Leung,[16] the fields within the photonic crystal in the presence of a defect are expanded in terms of vector Wannier functions. The application of exact Green's-function methods to the study of the defect modes in photonic crystals was also made by Maradudin and McGurn[17] for a two-dimensional periodic system formed from an array of cylindrical dielectric rods. The problem of a single dielectric-impurity rod or a cluster of rods with a general impurity dielectric constant in a truncated two-dimensional, periodic dielectric medium has been studied by Algul *et al.*[9] More recently, the Green's-function formalism has been applied to the study of a single impurity fabricated from a frequency-dependent material embedded in a photonic crystal formed from a frequency-independent material.[20]

In this paper, we focus on the study of the localized modes produced by introducing a defect cylinder into a two-dimensional periodic system consisting of parallel dielectric rods of circular cross section that are arrayed in a triangular lattice. It is well known that by changing the dielectric constant of a single cylinder one can create donor and acceptor states emerging from the top and the bottom of the gap. Alternatively, acceptor and donor levels may appear when the radius of a defect cylinder is reduced and increased, respectively. It has been demonstrated both theoretically and experimentally that the resulting acceptor defect creates a single level, while a donor defect creates multiple levels inside a band gap. Surprisingly, to date, to our knowledge, no systematic study of the symmetry of the defect modes and of the associated field patterns has been carried out, and this is the objective of this paper for the case of a triangular photonic crystal.

In our calculations, we apply a finite-difference time-domain technique developed within the framework of the supercell method, which allows calculating the eigenfrequency and the eigenfunction of a defect mode with high precision.[24] The method is based on the numerical simulation of the excitation of the defect mode by a virtual oscillating dipole located near the dielectric defect. By discretizing the inhomogeneous wave equation for the electric field in both space and time we have calculated the electric-field distribution, energy density, and electromagnetic energy emitted by the dipole as a function of frequency.

Our method fully allows for the satisfaction of the boundary conditions at the boundaries of the computational cell and, therefore, is applicable to the study of the uncoupled localized modes that cannot be excited by an external plane wave and have not been revealed by using conventional finite-difference techniques for calculating the transmission coefficient for the incident wave. Such information might be valuable in the design of photonic band-gap structures and devices in which these modes with eigenfrequencies within the higher-frequency gaps can be utilized or, on the other hand, if a single dominant mode is desired and modes of other symmetries are to be suppressed.

The present paper is organized as follows. In Sec. II we briefly describe the methods used in calculating the electromagnetic field radiated by an oscillating dipole embedded in a photonic crystal. In Sec. III we present results for the fully symmetric localized modes of A_1 symmetry of the C_{3v} point group for the system in which a single cylinder is removed from the center of the triangular lattice, which corresponds to the system studied experimentally in Ref. 14. Then we study the variation of the donor and acceptor levels that appear in the photonic band gap when the dielectric constant of a single cylinder and/or the radius of the defect rod is modified in a photonic crystal with two different values of the filling fraction of the rods. In Sec. IV we discuss and summarize the results obtained and give possible directions for future research.

II. METHODS OF CALCULATION

The numerical method used to calculate the eigenfrequency and eigenfunction of a defect mode in a triangular photonic crystal in this paper is based on the approach developed within the framework of the Green's-function formalism[24] that treats the inhomogeneous Maxwell's equations with a source term that is the extrinsic polarization field of an oscillating dipole embedded in the perfect photonic lattice. We solve this problem in the presence of the defect by using a numerical simulation of the excitation of the defect mode by an oscillating dipole located near the defect. Then by evaluating the electromagnetic energy emitted by the dipole as a function of frequency we determine the eigenfrequency of the defect mode as the resonance frequency.

We start from the following Maxwell's equations:

$$\nabla\times\mathbf{E}(\mathbf{x};t)=-\frac{1}{c}\frac{\partial}{\partial t}\mathbf{H}(\mathbf{x};t), \tag{2.1}$$

$$\nabla\times\mathbf{H}(\mathbf{x};t)=\frac{1}{c}\frac{\partial}{\partial t}\{\epsilon(\mathbf{x})\mathbf{E}(\mathbf{x};t)+4\pi\mathbf{P}_d(\mathbf{x};t)\}, \tag{2.2}$$

where $\epsilon(\mathbf{x})$ is a position-dependent dielectric constant that is a periodic function of $\mathbf{x}$, except for the disorder introduced by the dielectric defect, and $\mathbf{P}_d(\mathbf{x};t)$ is the polarization field of the oscillating dipole embedded in the photonic lattice, which can be written in the explicit form

$$\mathbf{P}_d(\mathbf{x};t)=\mathbf{d}_\mu\delta(\mathbf{x}-\mathbf{x}_0)\exp(-i\omega t), \tag{2.3}$$

where $\mathbf{d}_\mu$ is the amplitude of the oscillating dipole, $\mathbf{x}_0$ is the position vector of the dipole, and ω is the angular frequency of the oscillation.

The Green's-function method that treats the dipole radiation in a regular photonic lattice[24] can be applied to the problem of the calculation of the defect mode if the presence of the defect modes is taken into account in addition to the extended Bloch states. When we denote the eigenfunction and the eigenfrequency of the defect mode by $\mathbf{E}_d(\mathbf{x})$ and ω_d, assume that ω is close to ω_d, which is isolated in a photonic band gap, and neglect the contribution from all other eigenmodes, then Eq. (36) in Ref. 24 yields the following expression for the electric field of the present problem:

$$\mathbf{E}(\mathbf{x},t)\simeq-\frac{2\pi\omega_d\{\mathbf{d}_\mu\cdot\mathbf{E}_d^*(\mathbf{x}_0)\}\mathbf{E}_d(\mathbf{x})\exp(-i\omega t)}{V(\omega-\omega_d+i\Gamma)}, \tag{2.4}$$

where $\mathbf{E}_d(\mathbf{x})$ is normalized as

$$\int_V \epsilon(\mathbf{x})|\mathbf{E}_d(\mathbf{x})|^2 d\mathbf{x}=V. \tag{2.5}$$

In Eq. (2.4), Γ is a small positive constant that ensures the causality of the solution of Eqs. (2.1)–(2.2),[24] and V is the volume on which the cyclic boundary condition is imposed.

The electromagnetic energy U emitted per unit time by the oscillating dipole placed at $\mathbf{x}_0$ within the supercell is given by the surface integral of the normal component of the Poynting vector, which can be transformed into a volume integral by using Gauss's theorem. By calculating the Poynting vector and by using the normalization condition given by Eq. (2.5), we obtain the following expression for U:[25]

$$U=\frac{\pi\omega_d^2|\mathbf{d}_\mu\cdot\mathbf{E}_d(\mathbf{x}_0)|^2}{2V\{(\omega-\omega_d)^2+\Gamma^2\}}. \tag{2.6}$$

Then by evaluating the electromagnetic energy emitted by the dipole as a function of frequency we can obtain the eigenfrequency of the defect mode ω_d as a resonance frequency.

To perform this task, we use the numerical simulation of the dipole radiation to solve the inhomogeneous Maxwell's equations with a source term that is the extrinsic polarization field of the oscillating dipole given by Eq. (2.3). In this paper, we apply this technique to the problem of an isolated defect introduced into an otherwise perfect two-dimensional photonic crystal. The introduction of a defect into a periodic dielectric structure may give rise to localized states within the photonic band gap, which are donorlike or acceptorlike depending on the method used to form a defect. Specifically, we study the defect modes in a two-dimensional photonic lattice that consists of infinitely long parallel rods characterized by a dielectric constant ϵ_a embedded in a background dielectric material characterized by the dielectric constant ϵ_b. The rods are assumed to be parallel to the x_3 axis, and the intersections of the axes of the rods with a perpendicular plane form a two-dimensional triangular lattice. In particular, we are interested in exploring the nature of defect modes of C_{3v} symmetry, which may appear within the photonic gap when a cylinder is removed or an impurity cylinder with a modified dielectric constant is introduced into the otherwise perfect two-dimensional photonic crystal. We also study the alternative, technologically more favorable, defect states created by varying the radius of a single cylinder.

The vector electromagnetic field in the two-dimensional photonic lattice can be decoupled into two independent polarization components, i.e., E polarization for which the electric field is parallel to the rod axis, and H polarization for which the magnetic field is parallel to the rod axis.[7,26,27] In this paper, we will consider the particular case of the defect states of E polarization. The theory of the defect states of H polarization can be constructed along similar lines and will be presented elsewhere. The two-dimensional system we study is characterized by a dielectric constant of the form

$$\epsilon(\mathbf{x}_\parallel) = \epsilon_0(\mathbf{x}_\parallel) + \epsilon_d(\mathbf{x}_\parallel), \tag{2.7}$$

where $\epsilon_0(\mathbf{x}_\parallel)$ is a periodic function of $\mathbf{x}_\parallel$,

$$\epsilon_0[\mathbf{x}_\parallel + \mathbf{x}_\parallel(l)] = \epsilon_0(\mathbf{x}_\parallel), \tag{2.8}$$

where $\mathbf{x}_\parallel(l)$ is a translation vector of the triangular lattice, while $\epsilon_d(\mathbf{x}_\parallel)$ is nonzero in a small region of the x_1x_2 plane.

For the case of E polarization, the electric-field vector is given by

$$E(\mathbf{x};t) = (0,0,E_3(\mathbf{x}_\parallel;t)) \tag{2.9}$$

and

$$H(\mathbf{x};t) = (H_1(\mathbf{x}_\parallel;t), H_2(\mathbf{x}_\parallel;t), 0). \tag{2.10}$$

If we assume that the direction of the oscillating dipole moment $\mathbf{d}_\mu$ is parallel to the rods, and denote by (x_{10}, x_{20}) the position of the dipole moment within the x_1x_2 plane, Maxwell's equations for the amplitude functions $E_3(\mathbf{x}_\parallel;t)$, $H_1(\mathbf{x}_\parallel;t)$, and $H_2(\mathbf{x}_\parallel;t)$ take the form

$$\frac{\partial E_3}{\partial x_1} = \frac{1}{c}\frac{\partial}{\partial t} H_2, \tag{2.11}$$

$$\frac{\partial E_3}{\partial x_2} = -\frac{1}{c}\frac{\partial}{\partial t} H_1, \tag{2.12}$$

$$\frac{\partial H_2}{\partial x_1} - \frac{\partial H_1}{\partial x_2} = \frac{1}{c}\frac{\partial}{\partial t}\{\epsilon(\mathbf{x}_\parallel)E_3 + 4\pi d_\mu \delta(x_1 - x_{10}) \times \delta(x_2 - x_{20})\exp(-i\omega t)\}. \tag{2.13}$$

The equation for E_3 obtained by eliminating H_1 and H_2 can be written in the form

$$\left(\frac{\partial^2}{\partial x_1^2} + \frac{\partial^2}{\partial x_2^2}\right)E_3 - \frac{\epsilon(\mathbf{x}_\parallel)}{c^2}\frac{\partial^2}{\partial t^2}E_3 = \frac{\omega^2}{c^2} 4\pi d_\mu \delta(x_1 - x_{10})\,\delta(x_2 - x_{20})\exp(-i\omega t). \tag{2.14}$$

Now, by approximating both derivatives in space and time in the latter equation by finite differences, one obtains

$$\begin{aligned} E_{i,j}^{k+1} = {} & 2E_{i,j}^k - E_{i,j}^{k-1} + \frac{1}{\epsilon_{i,j}}\left(\frac{\Delta t}{\Delta x_1}\right)^2 [E_{i+1,j}^k + E_{i-1,j}^k - 2E_{i,j}^k] \\ & + \frac{1}{\epsilon_{i,j}}\left(\frac{\Delta t}{\Delta x_2}\right)^2 [E_{i,j+1}^k + E_{i,j-1}^k - 2E_{i,j}^k] \\ & + \frac{4\pi d_\mu}{\epsilon_{i,j}} (\omega\Delta t)^2 \delta_{ii0}\delta_{jj0} \exp(-i\omega t), \end{aligned} \tag{2.15}$$

where the index k refers to a grid point of time, the indices i and j denote the x_1 and x_2 axes, respectively, Δt is the division of time, and Δx_1, Δx_2 are the intervals between the neighboring nodes along the x_1 and x_2 axes, respectively, on a discrete two-dimensional mesh. To evaluate the electric field radiated from the oscillating dipole we solve Eq. (2.15) with the initial conditions $E_3(\mathbf{x}_\parallel;0) = 0$, $\partial E_3(\mathbf{x}_\parallel;0)/\partial t = 0$.

By using the values of the electric field obtained by solving Eq. (2.15) in a computational domain that is chosen to be a supercell composed of an array of 8×8 unit cells, we determine the components of the magnetic field from Eqs. (2.11) and (2.12). Then we use the components of the electric and magnetic fields to evaluate the frequency dependence of the electromagnetic energy emitted by the dipole per unit time, and we determine the frequency of the defect mode as the resonance frequency. The spatial distribution of the electric field with the frequency of the defect mode and the associated electromagnetic energy is sampled every $a/20$ in the region in the x_1x_2 plane consisting of 8×8 unit cells, each of which is characterized by the lattice constant a.

The fields at the nodes outside the computational domain are related to the field inside by imposing periodic boundary conditions. Modes within the domain investigated are excited by an oscillating dipole located near a defect cylinder in the photonic crystal, and the solution of Eq. (2.15) is carried out for enough dipole cycles until a converged eigenfrequency and a converged distribution of the electric field associated with the localized mode are achieved. The symmetry of the eigenmode can be specified by imposing periodic boundary conditions reflecting the symmetry of a particular irreducible representation of C_{3v} symmetry and by placing the dipole in an appropriate symmetrical configuration. Employing the symmetry of the C_{3v} point group leads to a large reduction of the computational task, since in fact the calculations for the defect modes that correspond to nondegenerate states were carried out in $\frac{1}{12}$ of the supercell. In order to discretize the wave equation we sampled the unit cell at a 20×20 mesh, and one period of oscillation was divided into 240 time points.

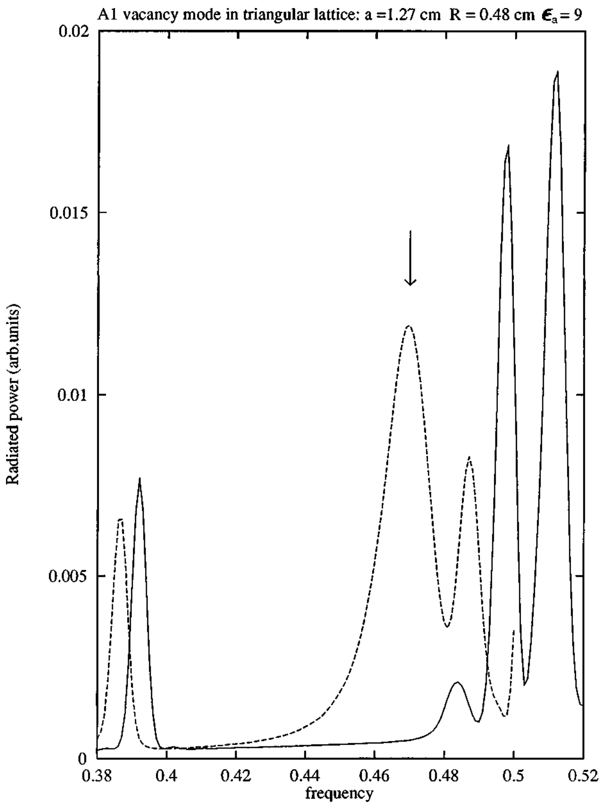

FIG. 1. The electromagnetic energy radiated by an oscillating dipole moment located at the center of the defect rod as a function of the oscillation frequency. The dashed curve corresponds to the configuration when a defect state is created by removing a single rod; the solid curve represents the radiated energy of an oscillating dipole in the perfect two-dimensional photonic crystal consisting of dielectric rods of circular cross section arrayed in a triangular lattice. As in the experimentally studied array of Smith *et al.* (Ref. 14), the following values were assumed: $a=1.27$ cm, $R=0.48$ cm, $\epsilon_a=9.0$, $\epsilon_b=\epsilon_d=1.04$. A resonance at $\omega a/2\pi c=0.471$ indicated by an arrow is clearly observed.

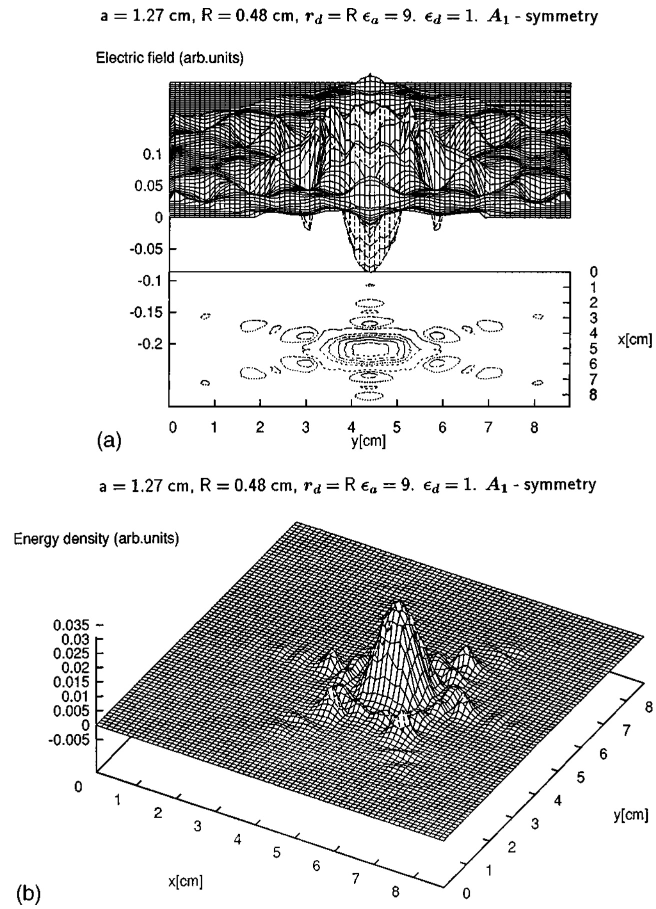

FIG. 2. The spatial distribution (a) of the electric field and (b) the energy density excited by the oscillating dipole after 100 cycles of oscillation at $\omega a/2\pi c=0.471$, which corresponds to the resonance shown in Fig. 1, caused by removing a single cylinder from the two-dimensional photonic crystal.

III. RESULTS

We first apply this method to the calculation of the totally symmetric A_1 mode of the C_{3v} point group, since the experimental observation of Smith *et al.* [Figs. 7(a) and 7(b) of Ref. 14] seems to show this symmetry. The experimental studies in Ref. 14 dealt with the defect configuration created by removing one cylinder from an otherwise perfect triangular photonic lattice with a lattice constant $a=1.27$ cm consisting of identical dielectric rods of radius $R=0.48$ cm, which corresponds to the filling fraction $f=0.518$, characterized by a dielectric constant $\epsilon_a=9$, embedded in a background dielectric material characterized by a dielectric constant $\epsilon_b=1.04$. Our motivation for performing the calculations in the system studied experimentally in Ref. 14 is twofold—to validate our approach in comparison with the experimental data and to examine the symmetry of the localized modes. In the following we focus on the study of the fully symmetric defect modes that possess the A_1 symmetry of the C_{3v} point group and we place the dipole at the origin, where the defect rod is centered. By imposing boundary conditions appropriate to the irreducible representations of the point group C_{3v}, and varying the dielectric strength of an impurity cylinder we have also found defect states of A_2, B_1, B_2, E_1, and E_2 symmetry. We will publish these results in a forthcoming paper.

It is well established that the photonic band structure for E-polarized electromagnetic waves propagating through the photonic crystal considered in Ref. 14 reveals several forbidden gaps. We are interested in the second lowest one, which appears in the frequency range $0.43<\omega a/2\pi c<0.49$, into which a defect state is introduced by removing a single cylinder from an otherwise perfect triangular photonic crystal. In Fig. 1, we present the electromagnetic energy radiated by an oscillating dipole located at the center of a defect rod versus frequency, which corresponds to a steady state after 100 cycles of oscillation. The calculated frequency dependence of the radiated power reveals a sharp resonance at $\omega a/2\pi c=0.471$. This peak is a consequence of a localized state of A_1 symmetry of the C_{3v} point group, and is in quantitative agreement with the experimentally observed transmission peak reported by Smith *et al.* in Ref. 14, which appears within the second-lowest band gap. The existence of the band gap is indicated in Fig. 1 by the solid curve that represents the radiated energy of an oscillating dipole in the perfect two-dimensional photonic crystal, and is in quantitative agreement with the results obtained by using a standard plane-wave technique.[27] The peaks centered at $\omega a/2\pi c$

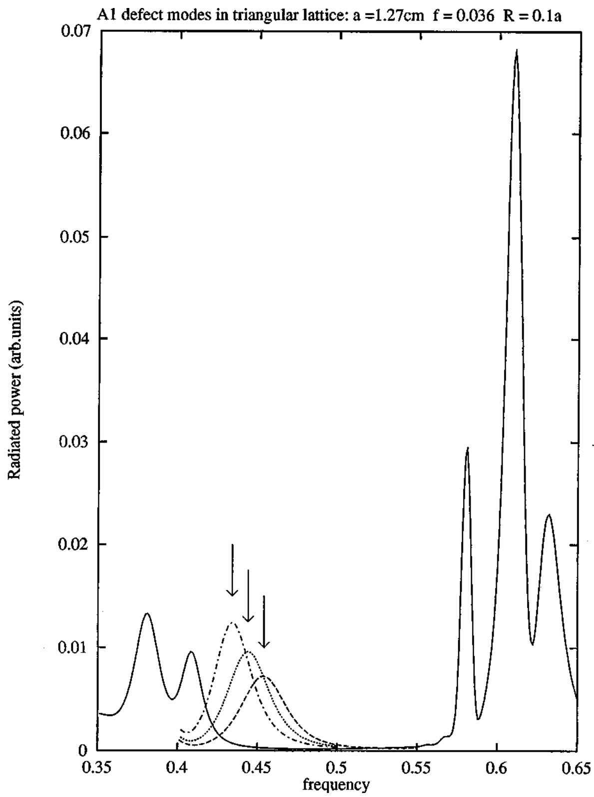

FIG. 3. The electromagnetic energy radiated by an oscillating dipole embedded in the supercell containing a defect with the radius $r_d = R$ for three values of the dielectric constant, viz., $\epsilon_d = 1$ (dashed curve) with the resonance at $\omega a/2\pi c = 0.456$, $\epsilon_d = 3$ (dotted curve) with the resonance at $\omega a/2\pi c = 0.446$, and $\epsilon_d = 5$ (dash-dotted curve) with the resonance at $\omega a/2\pi c = 0.436$. The solid curve represents the energy radiated by an oscillating dipole in the perfect two-dimensional photonic crystal when $\epsilon_a = 13$, $R = 0.1a$ $(f = 0.036)$, and $a = 1.27$ cm.

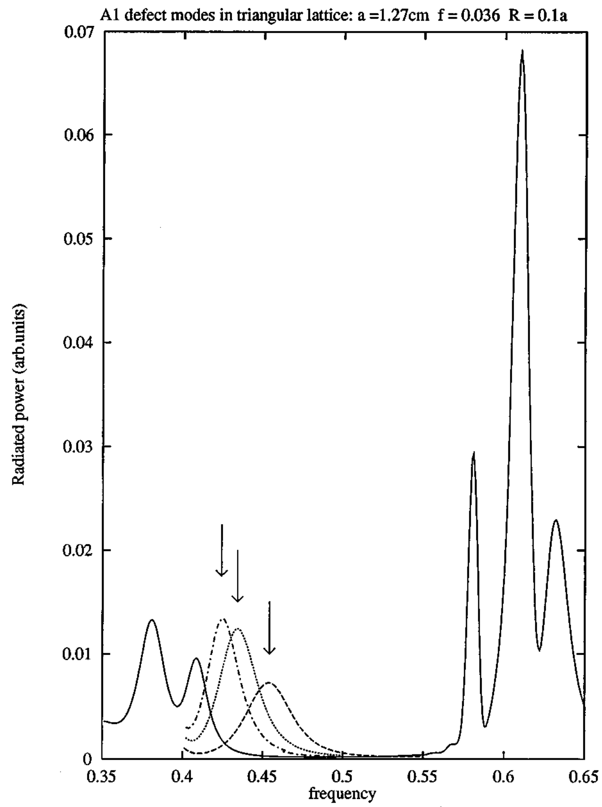

FIG. 4. The electromagnetic energy radiated by an oscillating dipole embedded in the supercell containing a defect rod with dielectric constant $\epsilon_d = 5$ when the radius of the rod is $r_d = R$ (dotted curve) with the resonance at $\omega a/2\pi c = 0.436$ and $r_d = 1.2R$ (dashed-dotted curve) with the resonance at $\omega a/2\pi c = 0.427$, compared with the corresponding result for a vacancy (dashed curve). The solid curve represents the energy radiated by an oscillating dipole in the perfect two-dimensional photonic crystal with the same parameters as in Fig. 3.

$= 0.39$ and 0.49 represent the onset of the continuum of the bands of A_1 symmetry at the lower and upper band edges, respectively. To verify the localized nature of the defect state we have evaluated the spatial distribution of the electric field. The field pattern and spatial distribution of the electromagnetic energy radiated by the oscillating dipole shown in Figs. 2(a) and 2(b), respectively, clearly demonstrate the rapid falloff of the energy density near the defect rod, as expected for a localized defect mode. Because the field pattern associated with this localized mode is strongly localized and has a vanishingly small amplitude at the boundary at $x = 4a$, a supercell composed of an array of 8×8 unit cells was found sufficient to achieve impurity-band-effect-free results. In addition, by placing the oscillating dipole at an off-defect-rod position at $x = (a,0)$ instead of at $x = (0,0)$, we obtained the identical field pattern and we demonstrated that the induced electromagnetic field belongs to a nondegenerate eigenmode. We have monitored the convergence of the eigenfrequencies obtained by using finer meshes in both space and time, and we have found that the frequencies are converged to better than 1%.

It is well known that when the dielectric strength of the defect rod is increased (decreased) a donor (acceptor) level may appear in the photonic band gap. The results displayed in Fig. 3 demonstrate the monotonic dependence of the defect levels on the variation of the dielectric strength of the defect rod in a system of rods of radius $R = 0.1a$, characterized by a dielectric constant $\epsilon_a = 13$, embedded in vacuum, that form a triangular lattice with the lattice constant $a = 1.27$ cm, which corresponds to a filling fraction $f = 0.036$. The photonic band structure for electromagnetic waves propagating through such a system reveals several photonic gaps. We focus on the lowest band gap that appears in the frequency range $0.42 < \omega a/2\pi c < 0.57$, which is indicated by the solid curve in Fig. 3. By varying the dielectric constant of the defect rod we have found resonances at the frequencies $\omega a/2\pi c = 0.456$, 0.446, and 0.436, which correspond to three values of the dielectric constant of the defect rod $\epsilon_d = 1$, $\epsilon_d = 3$, and $\epsilon_d = 5$, respectively. Both the electromagnetic-field distribution and the energy density associated with the defect state created by introducing an impurity rod characterized by a dielectric constant $\epsilon_d = 5$ display exponentially decaying spatial behavior that resemble the strongly localized nature of the defect mode shown in Figs. 2(a) and 2(b), respectively.

Varying the radius of the defect rod represents an alternative and technologically more favorable way of producing defect levels. The results shown in Fig. 4 illustrate how the position of the defect levels can be controlled by the simul-

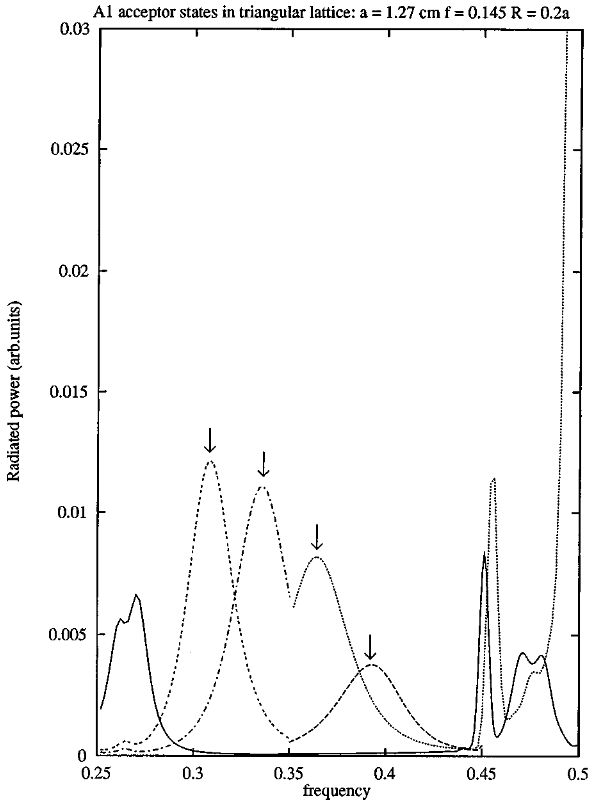

FIG. 5. The electromagnetic energy radiated by an oscillating dipole embedded in the supercell containing a defect rod characterized by the dielectric constant $\epsilon_d = 13$ for three values of the radius, viz., $r_d = 0.7R$ (dash-dashed curve) with the resonance at $\omega a/2\pi c = 0.310$, $r_d = 0.5R$ (dash-dotted curve) with the resonance at $\omega a/2\pi c = 0.338$, and $r_d = 0.3R$ (dotted curve) with the resonance at $\omega a/2\pi c = 0.367$, compared with the corresponding result for a vacancy (dashed curve), when $a = 1.27$ cm, $R = 0.2a$ ($f = 0.145$), and $\epsilon_a = 13$.

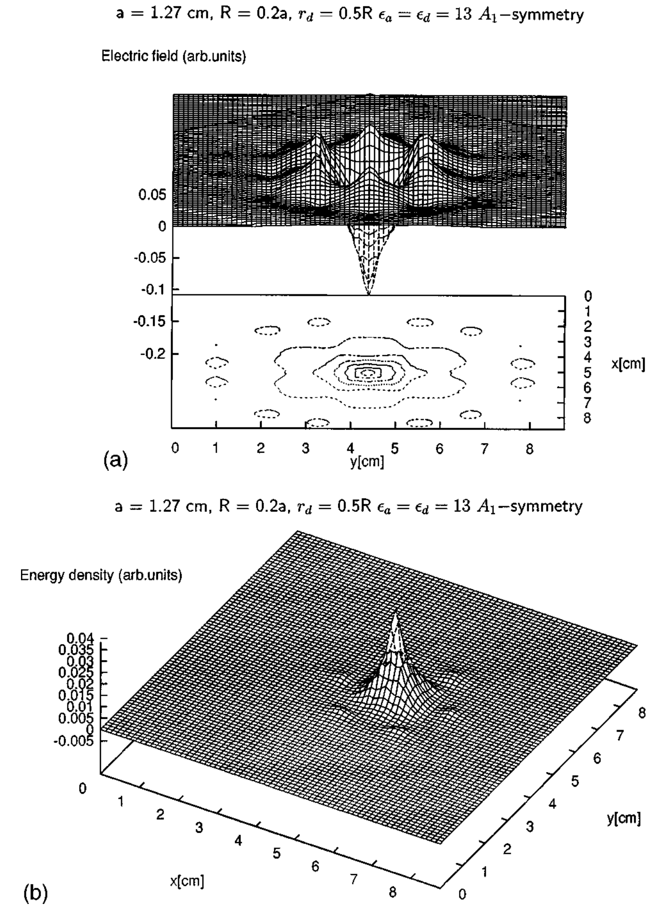

FIG. 6. The spatial distribution (a) of the electric field and (b) the energy density excited by the oscillating dipole after 100 cycles of oscillation at $\omega a/2\pi c = 0.338$, which corresponds to the defect state indicated by the dash-dotted curve in Fig. 5 produced by reducing the radius of the defect cylinder to $r_d = 0.5R$.

taneous variation of both the dielectric constant and the radius of the defect rod. We studied the dependence of the frequency associated with the defect level created by reducing the dielectric strength to $\epsilon_d = 5$ when the radius of the defect rod is increased in the range $R < r_d < 1.5R$. In Fig. 4, we display the resonances at the frequencies $\omega a/2\pi c = 0.436$ and 0.427, which correspond to the values of the radius of the defect rod $r_d = R$ and $r_d = 1.2R$, respectively. The frequencies associated with the defect modes shown in the latter figure decrease as the radius of the defect rod is increased. Such a variation of the defect level is consistent with the general result that by adding material to one of the unit cells the frequency of the defect level decreases. It resembles the tendency shown in Fig. 3, and confirms the equivalence of both methods of producing defect levels as alternative tools for controlling the position of the impurity level within the photonic gap. By evaluating the spatial distributions of the electric fields and energy densities associated with the defect levels indicated in Fig. 4, we confirmed their exponentially decaying behavior, which reflects the localized nature of the defect mode demonstrated in Figs. 2(a) and 2(b), respectively. Because the field associated with the localized modes presented in Figs. 3 and 4 has a vanishingly small amplitude at the boundary at $x = 4a$, a supercell composed of an array of 8×8 unit cells was found sufficient to achieve impurity-band-effect-free results. We have monitored the convergence of the eigenfrequencies obtained by using finer meshes in both space and time, and we have found that the frequencies are converged to better than 1%.

To demonstrate the efficiency and the capabilities of this method, we have also compared our results with the theoretical results of Ref. 23 obtained by the supercell method and the plane-wave approximation. In fact, we have studied the defect size dependence of the acceptor and donor levels in the system consisting of dielectric rods characterized by a dielectric constant $\epsilon_a = 13$ and radius $r_d = 0.2R$ embedded in vacuum, which form a triangular lattice with the lattice constant $a = 1.27$ cm that corresponds to the filling fraction $f = 0.145$. We have found that decreasing the radius of the defect cylinder in the range $0 < r_d < R$ gives rise to acceptor levels that penetrate into the gap from the continuum of the bands located below the bottom of the photonic band gap as indicated in Fig. 5. Specifically, we have found resonances at the frequencies $\omega a/2\pi c = 0.310$, 0.338, and 0.367, which correspond to the three values of the radius of the defect rod $r_d = 0.7R$, $r_d = 0.5R$, and $r_d = 0.3R$, respectively. In Figs. 6(a) and 6(b) we present the spatial distributions of the electric field and the energy density, respectively, associated with the defect rod with the radius reduced by $\Delta r_d = 0.5R$. Both quantities display exponentially decaying behavior,

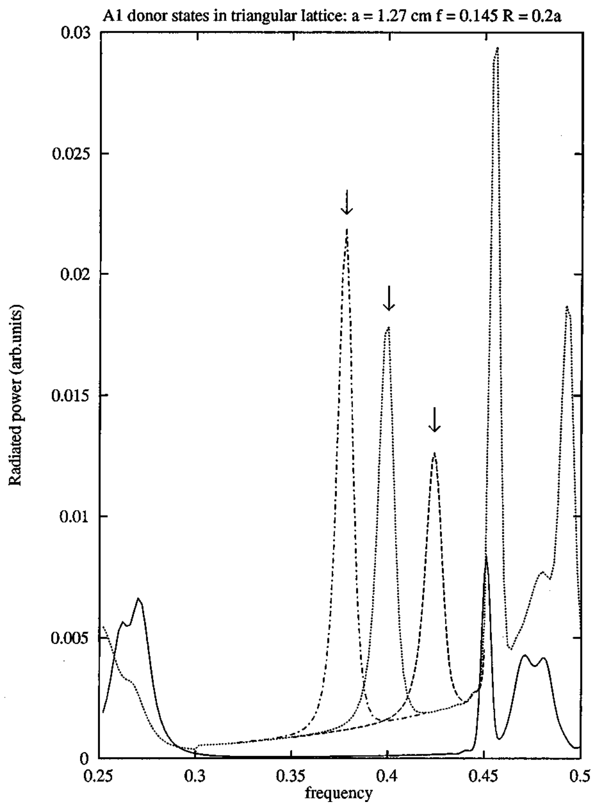

FIG. 7. The electromagnetic energy radiated by an oscillating dipole embedded in the supercell containing a defect rod with dielectric constant $\epsilon_d = 13$ when the radius of the rod is $r_d = 2.1R$ (dashed curve) with the resonance at $\omega a/2\pi c = 0.425$, $r_d = 2.3R$ (dotted curve) with the resonance at $\omega a/2\pi c = 0.40$, and $r_d = 2.5R$ (dash-dotted curve) with the resonance at $\omega a/2\pi c = 0.378$. The solid curve represents the energy radiated by an oscillating dipole in the perfect two-dimensional photonic crystal with the same parameters as in Fig. 5.

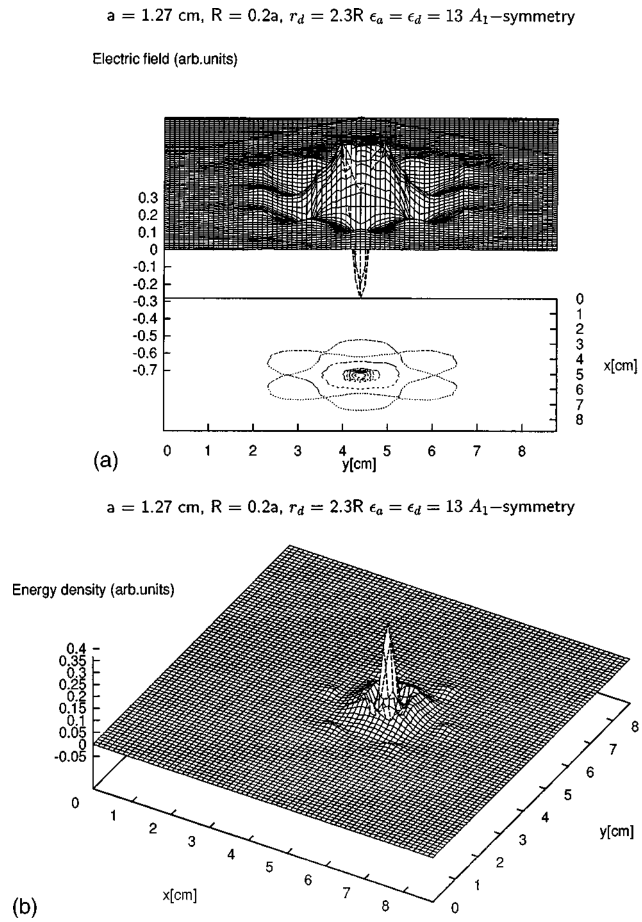

FIG. 8. The spatial distribution (a) of the electric field and (b) the energy density excited by the oscillating dipole after 100 cycles of the oscillation at $\omega a/2\pi c = 0.40$, which corresponds to the defect state indicated by the dash-dotted curve in Fig. 7 produced by increasing the radius of the defect cylinder to $r_d = 2.3R$.

which indicates the strongly localized nature of the acceptor mode. In order to study donorlike levels, we have increased the radius of a single cylinder and have confirmed the existence of defect levels that penetrate into the gap from the continuum of the bands located above the top of the photonic band gap. In Fig. 7, we depict the resonances associated with the donor defect modes made by increasing the radius of the defect cylinder in the range $2R < r_d < 2.5R$, namely, we display resonances at the frequencies $\omega a/2\pi c = 0.425$, 0.40, and 0.378, which correspond to the three values of the radius of the defect rod $r_d = 2.1R$, $r_d = 2.3R$, and $r_d = 2.5R$, respectively. The frequencies associated with the defect levels shown in Figs. 5 and 7 are in quantitative agreement with the nondegenerate acceptor and donor levels calculated for the identical system in Ref. 23. In Figs. 8(a) and 8(b), we display the distribution of the electromagnetic field and the energy density associated with the defect rod with the radius $r_d = 2.3R$, respectively. Both quantities display exponentially decaying amplitudes, and thus indicate the strongly localized nature of the donor mode. Both acceptor and donor levels appear within the lowest band gap in the frequency range $0.27 < \omega a/2\pi c < 0.45$, which is indicated by the solid curve in Figs. 5 and 7. The dependence of the radiated power of the dipole embedded in a perfect photonic crystal is in good quantitative agreement with the results for the photonic band structure for E-polarized electromagnetic waves propagating through such a system obtained by the standard plane-wave technique.

IV. DISCUSSION AND CONCLUSIONS

In this paper we have applied a finite-difference time-domain method developed within the framework of the supercell method and based on the numerical simulation of dipole radiation to a two-dimensional photonic crystal that consists of a triangular array of circular dielectric rods in which several types of defects are introduced. We first applied our method to the system with a single rod removed from the center studied experimentally by Smith *et al.*[14] The results obtained for this system are in excellent agreement with the measurements, and we have identified the experimentally observed localized mode located at 11.2 GHz as one of A_1 symmetry.

We have also examined systems in which the defect states are introduced by other methods, namely, by varying the dielectric strength of a single cylinder, by changing the defect size, and by a combination of both methods. Our results clearly indicate that by reducing or increasing the radius of the defect cylinder we can control the frequency of the defect state. This behavior is demonstrated by the appearance of acceptorlike levels that penetrate into the gap from the bottom of the band gap as the radius of the defect rod is reduced, and by the existence of donorlike levels that appear below the conduction-band edge when the radius of the defect rod is increased. The variation of the defect level caused by adding dielectric material to one of the unit cells displays the same tendency as its dependence on the dielectric strength of a single rod, and confirms the equivalence of both alternative methods of introducing the defect modes. To validate our method we have carried out a calculation of the defect size dependence in the configuration considered in Ref. 23, and we have found that our results for the defect states of A_1 symmetry are in very good quantitative agreement with the nondegenerate acceptor and donor levels reported in that work.

The results obtained demonstrate that our method constitutes a computationally viable technique, which yields accurate eigenvalues and eigenfunctions of the defect states and, therefore, a complete spatial mapping of the corresponding electric field in the system. As a reasonably simple alternative to computationally intensive schemes our method provides a theoretical tool that emulates an experimental measurement, which uses a tuned microwave probe, for example, and allows studying two- and three-dimensional systems. The method can be readily extended to the case of a line defect and can also be used for the investigation of surface modes. By imposing periodic boundary conditions reflecting the symmetry of irreducible representations of C_{3v} symmetry and by varying the dielectric strength and radius of the defect rod, our method allows predicting the frequencies of the defect states, which correspond to a particular irreducible representation. Then, if we consider the selection rules that apply to states with different symmetries as the origin of a feedback mechanism, we can use multilevel systems based on the photonic crystal technology as a source of stimulated emission. Studies in progress focus on the extension of the present method to the solution of the problem of frequency-dependent and nonlinear Kerr-like defects. In such systems, new physical phenomena are expected to occur.

In conclusion, we have successfully applied a finite-difference time-domain method to the study of isolated defects, which introduce strongly localized states within a forbidden gap of a photonic crystal. To demonstrate the efficiency of our approach we have studied the configuration with a single cylinder removed and the defect size dependence of the defect levels. The results obtained by our method are in very good quantitative agreement with the defect modes observed both experimentally and theoretically in earlier studies. In addition we have analyzed the variation of the defect levels with the size of a defect and its dielectric strength, and demonstrated the capability of the method to predict the dependence of the defect level on either of these parameters or on a combination of both methods for producing the defect level. By inspecting the spatial distribution of the electromagnetic field and the energy density we have verified the localized nature of the eigenfunctions associated with the defect states. In comparison with the supercell method using plane-wave expansions our approach does not suffer from slow convergence problems, and provides impurity-band-width-free results. In addition, it allows identifying the symmetry of the defect mode, and thus constitutes a viable computational method comparable to existing Green's-function techniques.

ACKNOWLEDGMENTS

The work of V.K. was supported by the Japanese Society for Promotion of Science and in part by Czech Academy of Sciences Grant No. 202/96/1239. V.K. wishes to thank the Research Institute for Electronic Science, Hokkaido University, for its hospitality during a visit, at which time this work was done. The work of A.A.M. was supported in part by NSF Grant No. DMR-9319404.

---

*Permanent address: Institute of Radio Engineering and Electronics, Czech Academy of Sciences, Chaberska 57, 182 51 Prague 8, Czech Republic.

[1] E. Yablonovitch, Phys. Rev. Lett. **58**, 2486 (1987).

[2] S. John, Phys. Rev. Lett. **58**, 2059 (1987).

[3] For recent reviews see the articles in *Photonic Band Gaps and Localization*, edited by C. M. Soukoulis (Plenum, New York, 1993); J. Opt. Soc. Am. B **10** (1993), special issue on Development and Applications of Materials Exhibiting Photonic Band Gaps, edited by C. M. Bowden, J. P. Dowling, and H. O. Everitt; J. Mod. Opt. **41** (1994), special issue on Photonic Band Structures, edited by G. Kurizki and J. W. Haus; in *Confined Electron and Photons*, Vol. 340 of *NATO Advanced Studies Institute, Series B Physics*, edited by E. Burstein and C. Weisbuch; and in *Band Gap Materials*, edited by C. M. Soukoulis (Kluwer, Dordrecht, 1996).

[4] J. D. Joannopoulos, R. D. Meade, and J. N. Winn, *Photonic Crystals, Molding the Flow of Light* (Princeton University Press, Princeton, NJ, 1995).

[5] K. M. Ho, C. T. Chan, and C. M. Soukoulis, Phys. Rev. Lett. **65**, 3152 (1990).

[6] For a recent review see P. L. Gourley, Nature (London) **371**, 571 (1994), and references therein.

[7] S. L. McCall, P. M. Platzman, R. Dalichaouch, D. Smith, and S. Schultz, Phys. Rev. Lett. **67**, 2017 (1991).

[8] R. Dalichaouch, J. P. Armstrong, S. Schultz, P. M. Platzman, and S. L. McCall, Nature (London) **354**, 53 (1991).

[9] W. Robertson, G. Arjavalingam, R. D. Meade, K. D. Brommer, A. M. Rappe, and J. D. Joannopoulos, Phys. Rev. Lett. **68**, 2023 (1992).

[10] E. Yablonovitch, T. J. Gmitter, R. D. Meade, A. M. Rappe, K. D. Brommer, and J. D. Joannopoulos, Phys. Rev. Lett. **67**, 3380 (1991).

[11] E. Yablonovitch, J. Opt. Soc. Am. B **10**, 283 (1993).

[12] R. D. Meade, K. D. Brommer, A. M. Rappe, and J. D. Joannopoulos, Phys. Rev. B **44**, 13 772 (1991).

[13] R. D. Meade, K. D. Brommer, A. M. Rappe, and J. D. Joannopoulos, Phys. Rev. B **48**, 8434 (1993).

[14] D. R. Smith, R. Dalichaouch, N. Kroll, S. Schultz, S. L. McCall, and P. M. Platzman, J. Opt. Soc. Am. B **10**, 314 (1993).

[15] D. R. Smith, N. Kroll, and S. Schultz, in *Photonic Band Gap Materials* (Ref. 3), p. 391.

[16] K. M. Leung, J. Opt. Soc. Am. B **10**, 303 (1993).

[17] A. A. Maradudin and A. R. McGurn, in *Photonic Band Gaps and Localization* (Ref. 3), p. 247.

[18] M. Sigalas, C. M. Soukoulis, E. N. Economou, C. T. Chan, and

K. M. Ho, Phys. Rev. B **48**, 14 121 (1993).
[19] H. G. Algul, M. Khazhinsky, A. R. McGurn, and J. Kapenga, J. Phys.: Condens. Matter **7**, 44 (1995).
[20] A. R. McGurn and M. Khazhinsky, in *Photonic Band Gap Materials* (Ref. 3), p. 487.
[21] E. Yablonovitch and D. E. Sievenpiper, Phys. Rev. Lett. **76**, 2480 (1996).
[22] C. T. Chan, Q. L. Yu, and K. M. Ho, Phys. Rev. B **51**, 16 635 (1995).
[23] X.-P. Feng and Y. Arakawa, Jpn. J. Appl. Phys., Part 2 **36**, L122 (1997).
[24] K. Sakoda and K. Ohtaka, Phys. Rev. B **54**, 5732 (1996).
[25] K. Sakoda, T. Ueta, and K. Ohtaka, Phys. Rev. B **56**, 14 905 (1997).
[26] P. R. Villeneuve and M. Piché, Phys. Rev. B **46**, 4969 (1992).
[27] M. Plihal and A. A. Maradudin, Phys. Rev. B **44**, 8565 (1991).